Submitted for the proceedings of the 2016 ESA Living Planet Symposium held in Prague, Czech Republic, 9-13 May 2016, ESA Special Publication SP-740

OCEAN COLOUR REMOTE SENSING OF EXTREME CASE-2 WATERS

Martin Hieronymi [(1)], Hajo Krasemann [(1)], Dagmar Müller [(1)], Carsten Brockmann [(2)], Ana Ruescas [(2)], Kerstin Stelzer [(2)], Bouchra Nechad [(3)], Kevin Ruddick [(3)], Stefan Simis [(4)], Gavin Tilstone [(4)], François Steinmetz [(5)], Peter Regner [(6)]

[(1)] *Helmholtz-Zentrum Geesthacht (HZG), Institute of Coastal Research, Max-Planck-Str. 1, 21502 Geesthacht, Germany, martin.hieronymi@hzg.de*

[(2)] *Brockmann Consult GmbH (BC), Max-Planck-Str. 2, 21502 Geesthacht, Germany*

[(3)] *Royal Belgian Institute of Natural Sciences (RBINS), Operational Directorate Natural Environment, 100 Gulledelle, 1200 Brussels, Belgium*

[(4)] *Plymouth Marine Laboratory (PML), Prospect Place, Plymouth PL1 3DH, United Kingdom*

[(5)] *HYGEOS, Euratechnologies, 165 Avenue de Bretagne, 59000 Lille, France*

[(6)] *European Space Agency (ESA), ESRIN, Via Galileo Galilei, 00044 Frascati, Italy*

ABSTRACT

Many coastal seas and inland waters have water properties which are outside the normal conditions used for ocean colour algorithm design. In the ESA-funded "Case-2 Extreme" project, retrieval methods for OC products in extreme Case-2 waters are developed, tested, implemented, and validated primarily with reference to the capabilities of the Sentinel-3 OLCI and SLSTR instruments but also tested for Sentinel 2 where applicable. Based on hyperspectral radiative transfer simulation, *in situ*, and Earth observation data, specific features of extreme scattering and absorbing waters are reviewed. A reflectance-based sub-classification scheme of Case-2 waters for various levels of turbidity is introduced. Opportunities of using new wavebands are highlighted.

1. INTRODUCTION

Two water classes are typically distinguished in Ocean Colour remote sensing. Case-1 describes water in the open ocean where optically active constituents of seawater are determined only by phytoplankton and its co-varying detritus and coloured dissolved organic matter (CDOM); all other water types are covered by Case-2 (C2) [1]. Near coasts the water is generally more optically complex due to river input of CDOM and sediments, and resuspension of particulate matter in shallow waters. However, further differentiations of Case-2 waters can be made from an optical point of view. CDOM absorbs exponentially with decreasing wavelength in the visible range and does not scatter light. With high CDOM concentrations we may define the case of highly absorbing waters, decreasing the intensity of water-leaving radiance and yielding absorption overlap with phytoplankton pigments. Suspended particulate matter (SPM) absorbs and scatters light, both exponentially in the visible spectral range, while scattering dominates the total attenuation of light in the near infrared (NIR). In the presence of high SPM concentrations, we speak of highly scattering waters.

Highly absorbing and scattering waters are mostly found in coastal areas, marginal seas, inland waters and estuaries. Fig. 1 shows selected regions of interest: highly scattering waters can be found for example along the Belgian coast or the river mouth of the Río de la Plata, highly absorbing waters include the Lena Delta, Baltic Sea, and many lakes.

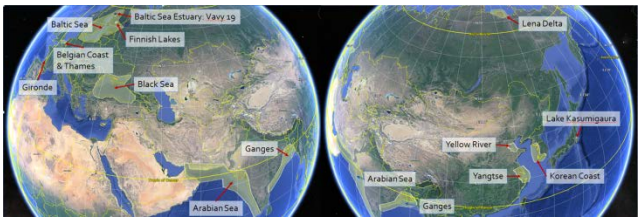

Figure 1. Regions of interest with extreme Case-2 waters.

The objective of the ESA project "Extreme Case-2 Waters" (C2X) is to study, implement, and validate existing atmospheric correction (AC) algorithms and water constituent retrieval in extremely absorbing and/or scattering Case-2 waters and – if possible – advance these remote sensing methods. The research focus is on the

Sentinel-3 mission with possible synergy of the OLCI and SLSTR instruments. Sentinel-2, ENVISAT/MERIS, and other missions are under consideration too and act as development platform as long as Sentinel-3 data is still not available. At the end of the project (2017) the selected C2X processors will be available in the ESA open source Sentinel toolbox SNAP.

Several algorithms are tested using Earth observation, *in situ*, and simulated data. The present paper focusses on the radiative transfer simulations. Information on some algorithms under consideration can be found in companion papers, e.g. the SWIR-based atmospheric correction used for Landsat-8 and Sentinel-2, which may be adapted within the Case2X project for the combined OLCI/SLSTR spectrum [2-4].

2. RADIATIVE TRANSFER SIMULATIONS

2.1. IN-WATER SIMULATION

Numerous in-water radiative transfer simulations have been carried out using the Hydrolight HE5.2 software [5]. The spectral range covers the full visible range, NIR up to 1100 nm, and the three SLSTR SWIR bands. A variety of water types were tested ranging from very clear to extremely scattering or absorbing cases. Based on simulated remote sensing reflectance R_{rs}, which is the ratio of water-leaving radiance to downwelling irradiance above the sea surface, differentiation features for various water types are introduced. Here, R_{rs} refers to clear atmosphere with Sun at zenith and viewing angle exactly perpendicular.

OLCI covers the same spectral bands as MERIS but with six additional bands. In particular the new bands at 400 and 1020 nm are relevant here. The MERIS and new OLCI bands are marked in Fig. 2, which shows typical R_{rs} spectra of Case-1, Case-2 scattering, and extremely scattering waters. Sub-classifications in terms of SPM (including organic and inorganic particles), particulate backscattering (b_{bp}) at 555 nm, and R_{rs} at different NIR wavebands is provided in Tab.1. In comparison to Case-1, there is non-zero reflectance in the NIR. The reflectance of the OLCI band at 1020 nm will be non-zero for extremely turbid waters, whereas the two AC-usable SLSTR SWIR bands will have negligible water reflectance even for the highest SPM concentrations [6-7].

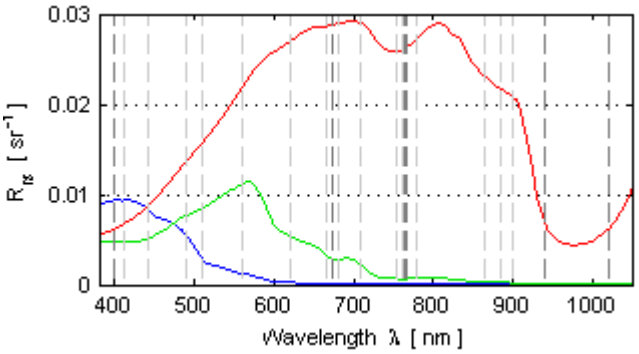

Figure 2. Remote sensing reflectance spectra of typical Case-1 (blue curve), Case-2 scattering (green curve), and extremely scattering (red curve) waters. The MERIS and new OLCI bands are marked with light and dark grey dashed lines.

Table 1. Sub-classification of Case-2 scattering (C2S) and extremely scattering (C2SX) waters.

	Case-1	C2S	C2SX
SPM [g m^{-3}]	< 1	1 – 100	> 100
a_{dg} (412) [m^{-1}]	< 0.58	0.08 – 8.46	> 8
b_{bp} (510) [m^{-1}]	< 0.025	0.0095 – 1.039	> 1
R_{rs} (780) [sr^{-1}]	$< 2.9 \cdot 10^{-4}$	$1.2 \cdot 10^{-4} – 0.0118$	> 0.0096
R_{rs} (865) [sr^{-1}]	$< 1.2 \cdot 10^{-4}$	$4.9 \cdot 10^{-5} – 0.0054$	> 0.0049
R_{rs} (1020) [sr^{-1}]	$< 1.8 \cdot 10^{-5}$	$6.8 \cdot 10^{-6} – 8.9 \cdot 10^{-4}$	$> 7.4 \cdot 10^{-4}$

Highly absorbing waters are characterized by very low water-leaving radiance. They may even be referred to as black waters. The maximum of R_{rs} is typically < 0.005 sr^{-1} and located between 550 and 605 nm for Case-2 absorbing (C2A) cases. For extremely absorbing waters (C2AX), the maximum shifts towards the red spectral range > 600 nm. Examples of C2A and C2AX are illustrated in Fig. 3. The definitions for absorbing waters are subject to ambiguities depending on the amount of scattering material. Simulated R_{rs} spectra are significantly changed if inelastic scattering, such as fluorescence of chlorophyll and CDOM as well as Raman scattering (by water molecules), is taken into account. Fluorescence quantum efficiency exhibits species-specific, seasonal, diurnal, and physiological variability, whereas it is fixed in the Hydrolight simulations [8]. Sun-induced chlorophyll-*a* fluorescence yields a peak around 685 nm. Depending on the concentration of chlorophyll-*a*, the simulated data include cases where the fluorescence

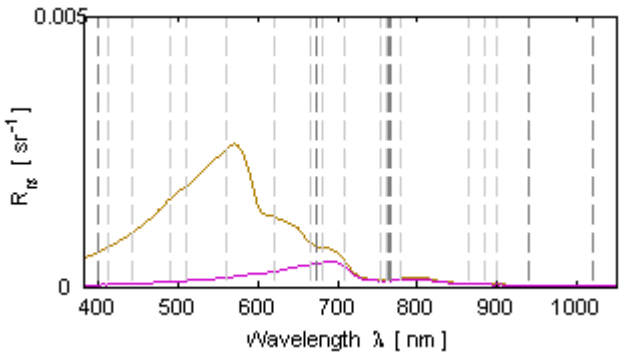

Figure 3. R_{rs} of Case-2 absorbing (brown curve) and extremely absorbing (purple curve) waters.

peak exceeds the R_{rs} maximum. In the simulations, CDOM fluorescence also affects the spectral shape of R_{rs} in the entire visible range and is particularly influential for high CDOM concentrations in conjunction with low chlorophyll concentrations. However, *in situ* data of extremely absorbing waters do not show marked CDOM fluorescence shapes of R_{rs}. Some caution interpreting the simulated spectra which include inelastic scattering is therefore advised. Regarding ambiguities with Case-1 waters, the OLCI band at 400 nm enables better differentiation of absorbing waters because high CDOM absorption results in very low R_{rs} (400) mostly below 0.001 (Fig. 4).

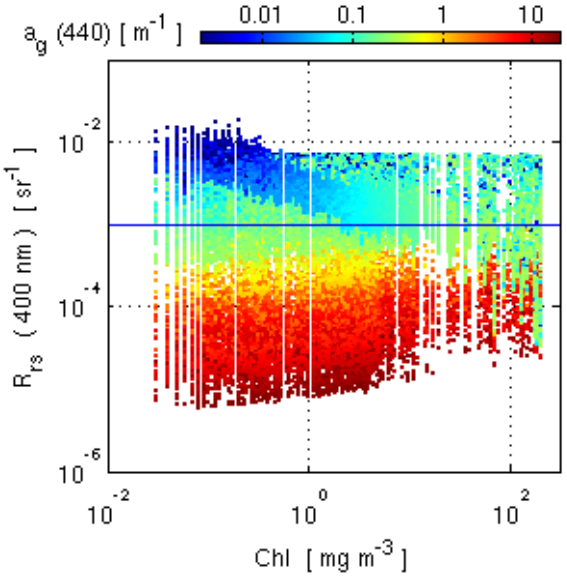

Figure 4. Remote sensing reflectance at 400 nm of all simulations vs. chlorophyll-a concentration. Colours indicate the CDOM absorption a_g at 440 nm.

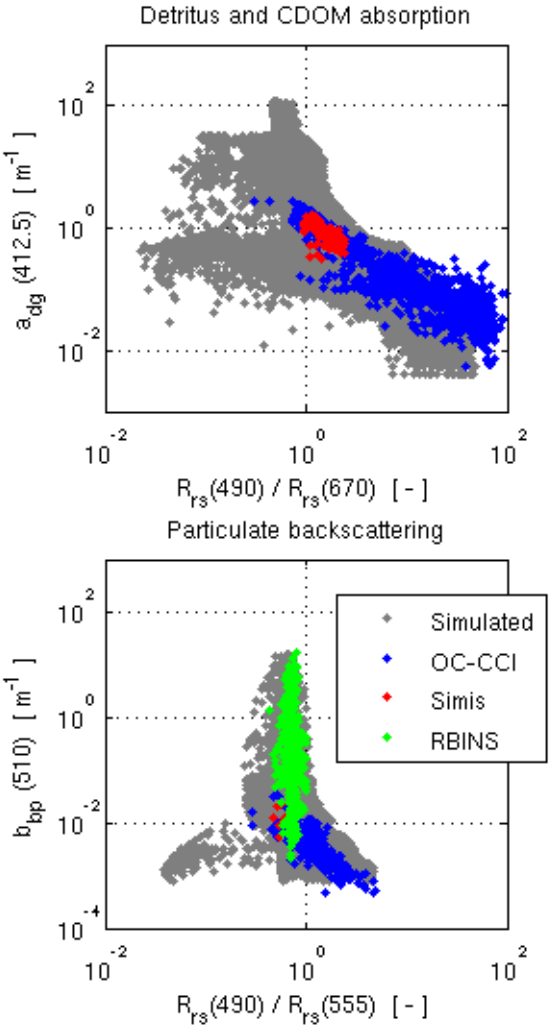

Figure 5. Comparison of simulated data (with and without inelastic scattering) with different in situ data. Top: Band ratio 490/670 vs. combined absorption of detritus and CDOM at 412.5 nm. Below: Band ratio 490/555 vs. particulate backscattering at 510 nm.

2.2. ATMOSPHERIC CORRECTION

Atmospheric correction (AC) is crucial for all extreme waters. The challenge is to deal with very bright pixels over scattering waters, in particular in the NIR, and very dark pixels of absorbing waters. Different AC methods are tested for C2X waters regarding their performance under various water types and atmospheric conditions.

Radiative transfer simulations have been performed using irradiance reflectance just below the surface from in-water

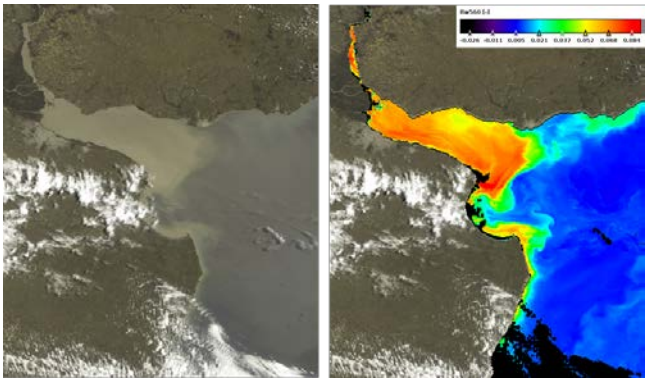

Figure 6. Left: MERIS RGB composite of Río de la Plata (acquired 2007-12-08) with sun glint reflectance of 9 %. Right: Water reflectance at 560 nm retrieved by Polymer.

Hydrolight simulations as lower boundary to the Monte-Carlo code SMART-G (developed by HYGEOS) providing the top-of-atmosphere signal. These simulations use various atmospheric conditions, including perturbations by aerosols, adjacency effect and sun glint. The simulations are used to study and enhance the performance of AC methods such as Polymer. The benefit from the addition of OLCI bands at 400 and 1020 nm and SLSTR SWIR bands on the AC is also assessed. An example of atmospheric correction with Polymer is provided in Fig. 6.

3. OPTICAL WATER CLASSES

Fifteen optical water classes can be defined on the simulated reflectance at SeaWiFS wavelengths [9]. The classification is applied to the OC-CCI dataset, which comprises merged satellite data at the SeaWiFS bands with 4 km x 4 km resolution. Fig. 7 shows the distribution of water classes in the North and Baltic Sea based on averaged reflectance over one month (June 2005). Maximum membership of Case-1 waters is illustrated with green colours, bluish and red tones represent absorbing (C2A and C2AX) waters, and grey-yellow indicates scattering (C2S and C2SX) waters. The water classes can be used to adapt and choose water constituent retrievals, but they are sensitive to the validity of the atmospheric correction.

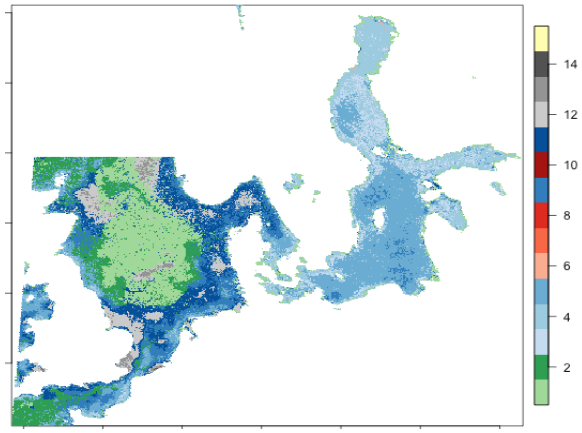

Figure 7. Regional distribution of optical water classes in North and Baltic Sea based on merged and monthly averaged OC-CCI data v2 from June 2005.

4. CONCLUSIONS

In terms of the appropriate choice of OC processors (atmospheric correction and in-water retrieval) it is useful to distinguish absorbing and scattering waters as well as their extremes. Sub-classifications of optical complex Case-2 waters are introduced based on inherent optical properties and remote sensing reflectance. The new Sentinel-3/OLCI and SLSTR bands provide tools for increasing the performance of atmospheric correction over extreme waters and for better identification of water types; NIR and SWIR bands for scattering waters and the 400 nm band for absorbing waters.

5. ACKNOWLEDGEMENTS

This work has been carried out in the framework of the ESA-funded “Case-2 Extreme” (C2X) project, within the SEOM Programme (Scientific Exploitation of Operational Missions, SEOM-DTEX-EOPS-SW-14-0002). Baltic Sea reflectance spectra were obtained through BONUS project FerryScope (www.ferryscope.org). Martin Hieronymi is supported through an ESA Living Planet Fellowship.

6. REFERENCEES

1. Morel, A. & Prieur, L. (1977). Analysis of variations in ocean color. *Limnol. Oceanogr*. **22**(4), 709-722.

2. Vanhellemont Q. & Ruddick K. (2015). Advantages of high quality SWIR bands for ocean colour

processing: Examples from Landsat-8, *Remote Sens. Environ.* 161, 89–106.

3. Brockmann, C & Doerffer, R. (2016). Evolution of the C2RCC neural network for Sentinel 2 and 3 for the retrieval of ocean colour products in normal and extreme optically complex waters. *Proc. Living Planet Symposium*, ESA SP-470.

4. Hieronymi, M., Müller, D., Krasemann, H., Schönfeld, W., Röttgers, R., & Doerffer, R. (2015). Regional ocean colour remote sensing algorithm for the Baltic Sea. *Proc. Sentinel-3 Science Workshop*, ESA SP-734.

5. Mobley, C. (1994). *Light and water: radiative transfer in natural waters*. Academic press.

6. Knaeps, E., Dogliotti, A. I., Raymaekers, D., Ruddick, K. & Sterckx, S. (2012) In situ evidence of non-zero reflectance in the OLCI 1020nm band for a turbid estuary, *Remote Sen. Environ.* 120, 133–144.

7. Ruddick, K. & Vanhellemont, Q. (2015). Use of the new OLCI and SLSTR Band for Atmospheric Correction over Turbid Coastal and Inland Waters, *Proc. Sentinel-3 Science Workshop*, ESA SP-734.

8. Greene, R. M., Kolber, Z. S., Swift, D. G., Tindale, N. W. & Falkowski, P. G. (1994). Physiological limitation of phytoplankton photosynthesis in the eastern equatorial Pacific determined from variability in the quantum yield of fluorescence. *Limnol. Oceanogr*. **39**(5), 1061-1074.

9. Moore, T. S., Campbell, J. W., & Feng, H. (2001). A fuzzy logic classification scheme for selecting and blending satellite ocean color algorithms. *IEEE Trans. Geosci. Remote Sens.* 39(8), 1764-1776.